doi:10.1246/cl.2012.1009
Published on the web September 8, 2012

Solution-phase Synthesis of Stannite-type Ag_2ZnSnS_4 Nanoparticles for Application to Photoelectrode Materials

Tetsuya Sasamura,[1] Takaaki Osaki,[1] Tatsuya Kameyama,[1] Tamaki Shibayama,[2] Akihiko Kudo,[3] Susumu Kuwabata,[4] and Tsukasa Torimoto*[1]

[1]*Department of Crystalline Materials Science, Graduate School of Engineering, Nagoya University, Chikusa-ku, Nagoya, Aichi 464-8603*

[2]*Center for Advanced Research of Energy Conversion Materials, Hokkaido University, Sapporo, Hokkaido 060-8628*

[3]*Department of Applied Chemistry, Faculty of Science, Tokyo University of Science, 1-3 Kagurazaka, Shinjuku-ku, Tokyo 162-8601*

[4]*Department of Applied Chemistry, Graduate School of Engineering, Osaka University, Suita, Osaka 565-0871*

(Received July 13, 2012; CL-120751; E-mail: torimoto@apchem.nagoya-u.ac.jp)

Ag_2ZnSnS_4 (AZTS) nanoparticles were successfully synthesized at relatively low temperature via thermal reaction of corresponding metal acetates and a sulfur source in a hot oleylamine solution, the purity of the particles being dependent on the amount of metal acetates and the reaction temperature. The obtained pure AZTS particles with size of ca. 15 nm exhibited photoresponse with visible light irradiation similar to that of n-type semiconductors.

Semiconductor nanoparticles (quantum dots), such as PbS, CdSe, and CdTe nanoparticles, exhibit tunable optical and electric properties, depending on their chemical composition, size, and shape, and have attracted a great deal of attention for applications to fluorescent markers, biosensors, optoelectric devices, and quantum dot solar cells.[1–15] Recent development in wet chemical syntheses has enabled the preparation of nanoparticles of Cu-based I–II–IV–VI of Cu_2ZnSnS_4 (CZTS) having a stannite-type crystal structure, which are promising materials as light absorbers in the next-generation photovoltaic devices because of the direct band gap semiconductor having a high absorption coefficient and consisting of only low toxic and abundant elements.[16–21]

We reported in our previous paper[22] that bulk I–II–IV–VI semiconductor particles, prepared via solid-state synthesis at relatively high reaction temperatures of 450–550 °C, acted as visible-light-driven photocatalysts. Photocatalytic activities for hydrogen generation were higher for Ag-based semiconductor particles, such as Ag_2ZnSnS_4 (AZTS), Ag_2ZnGeS_4, and their solid solution, than that observed for CZTS. Among them, the AZTS particles were one of the most active photocatalysts, because they had relatively high potential of the conduction band edge and were photoexcited with the visible light irradiation due to their band gap of 2.0 eV. Considering these results, it is also expected that nanoparticles of AZTS would be promising light-absorbing materials for photovoltaic devices, such as quantum dot solar cells. However, to the best of our knowledge, there has been no attempt to prepare AZTS particles in the nanometer region, though many strategies have been developed for the syntheses of Cu-based I–II–IV–VI semiconductor nanoparticles.

Here, we report for the first time the synthesis of colloidal AZTS nanoparticles through thermal reactions of corresponding metal acetates and a sulfur source in a hot oleylamine solution. The electronic energy structure of the particles was clarified by photoelectrochemical measurement of AZTS-immobilized electrodes.

AZTS nanoparticles were synthesized through thermal reactions in a hot oleylamine solution. A 0.20 mmol portion of ammonium *N*,*N*-diethyldithiocarbamate was dissolved in 1.0 cm^3 of oleylamine at 60 °C. After cooling the solution, a 2.0 cm^3 portion of oleylamine containing $AgCH_3COO$ (0.10 mmol), $Zn(CH_3COO)_2$, and $Sn(CH_3COO)_4$ (0.050 mmol) was added to the solution. The concentration of Zn precursor was varied in such a way that the ratio of Ag:Zn:Sn in the preparation was $2:R_{Zn}:1$ ($R_{Zn} = 0.5$–2). The resulting oleylamine solution was heat-treated at various temperatures (250–350 °C) for 10 min in an N_2 atmosphere. Thus-obtained precipitates were isolated by centrifugation, followed by washing with methanol several times and then dissolving in chloroform for measurements. The AZTS particles were accumulated on ITO substrates (sheet resistance: 10 Ω/□) by the previously reported layer-by-layer deposition technique with the use of 1,2-ethanedithiol (EDT).[23] The accumulation cycles were repeated five times. The obtained particle films were heat-treated at 200 °C for 10 min under vacuum to remove EDT for improving the electric connection between particles before the electrochemical measurements. Crystal structures of the obtained particles were analyzed using powder X-ray diffraction (XRD) (Rigaku, 2100HL) with Cu Kα radiation ($\lambda = 1.54059$ Å).

The reaction temperature for synthesis greatly affected the size and shape of the resulting nanoparticles and their chemical composition. Figures 1a and 1b show TEM images of nanoparticles obtained at 250 and 350 °C with the ratio of Ag:Zn:Sn = 2:1:1 ($R_{Zn} = 1.0$). Regardless of the reaction temperature, two kinds of particles were observed: spheres or polygons with darker contrast and rods having large aspect ratios. Selected-area EDX analyses (Figure S1[26]) revealed that rod-shaped particles contained only elements of Zn and S, being ZnS particles, while the spherical particles were composed of Ag, Zn, Sn, and S elements. These results indicated that a mixture of particles having different chemical compositions was formed in the preparation with $R_{Zn} = 1.0$.

Particles were prepared at the temperature of 350 °C with different value of R_{Zn} for investigating the influence of Zn content in the preparation on purity of the resulting particles. The rod-shaped particles, contained in samples prepared with R_{Zn} of 1.0–2.0 (Figures 1b and S2[26]), disappeared in the particles synthesized with $R_{Zn} = 0.75$, and then nanoparticles having polygonal or spherical shapes (Figure 1c) were observed

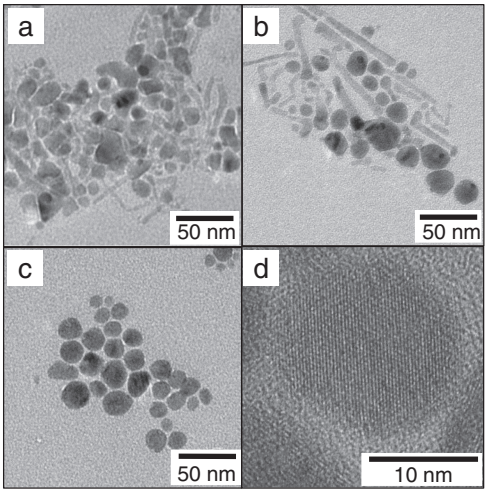

Figure 1. TEM images of particles synthesized at 250 (a) and 350 °C with $R_{Zn} = 1.0$ (b) and at 350 °C with $R_{Zn} = 0.75$ (c, d). Image d is a high-resolution image of the same sample in image c.

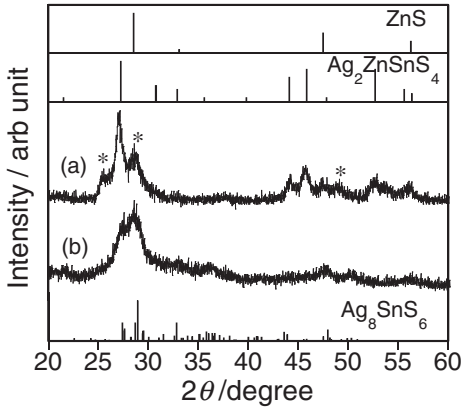

Figure 2. XRD patterns of obtained nanoparticles prepared at 350 °C with $R_{Zn} = 0.75$ (a) and at 250 °C with $R_{Zn} = 1.0$ (b). Unidentified peaks are marked with asterisks. Reference patterns of Ag_8SnS_6, tetragonal Ag_2ZnSnS_4, and cubic ZnS are also shown.

with a wide size distribution (average size of 15 nm and standard deviation of 4.4 nm). A high-resolution TEM image of the spherical particles prepared at $R_{Zn} = 0.75$ is shown in Figure 1d. Continuous lattice fringes appeared throughout the particle without lattice defects, indicating that the particle was made of a single crystal. Lattice spacings were 0.32 nm, being assigned to the (112) plane of tetragonal AZTS. EDX analyses revealed that the particles prepared at $R_{Zn} = 0.75$ contained metal elements with Ag:Zn:Sn = 1.60:1.14:1.0, the Ag content being slightly smaller than the theoretical value of Ag:Zn:Sn ratio (2:1:1) for Ag_2ZnSnS_4.

Figure 2 shows XRD patterns of thus-obtained particles. The sample prepared at 350 °C with R_{Zn}= 0.75, which contained no rod-shaped particles, exhibited a diffraction pattern mainly corresponding to tetragonal AZTS phase (Figure 2a), but unidentified small peaks at 25.5, 28.5, and 49.0° were also observed in the diffraction pattern, which did not accurately

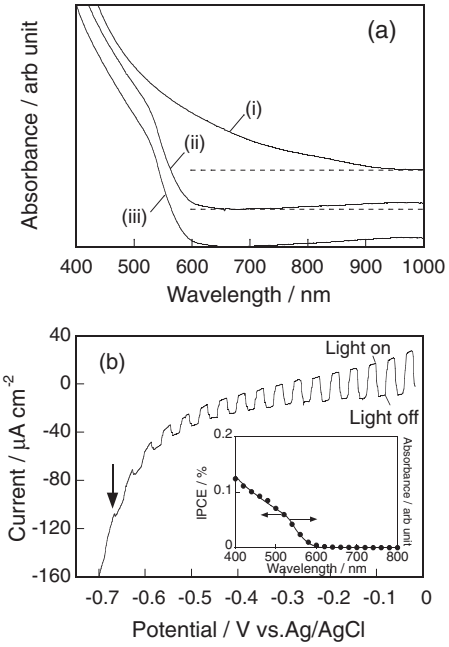

Figure 3. (a) Absorption spectra of nanoparticles prepared at 250 (i) and 350 °C with $R_{Zn} = 1.0$ (ii) and at 350 °C with $R_{Zn} = 0.75$ (iii) dissolved in chloroform. (b) Photocurrent–potential curve of an AZTS-immobilized ITO electrode. AZTS particles used were prepared at 350 °C with $R_{Zn} = 0.75$. (Inset) photocurrent action spectrum obtained at +0.5 V vs. Ag/AgCl.

agree with any JCPDS standard patterns of compounds consisting of Ag, Zn, Sn, or S, such as ZnS, and Ag_8SnS_6. So far there has been no report for obtaining a wurtzite-type (orthorhombic) AZTS crystal, but it is theoretically predicted that the wurtzite-type crystal structure was also stable for AZTS as well as the tetragonal structure, and synthesis of such a crystal structure has been reported only for $Ag_2CdSnSe_4$ among Ag-based I–II–IV–VI materials.[24] Therefore, it is suggested from these facts and XRD results in Figure 2 that a small amount of wurtzite-type AZTS nanocrystal was contained in the obtained particles of tetragonal AZTS phase. On the other hand, the particles prepared at 250 °C exhibited broad diffraction peaks around 27.3, 28.5, 36.0, and 47.6° that were assignable to Ag_8SnS_6 or ZnS crystal structures. These indicated that the low reaction temperature did not produce an AZTS crystal structure, being in good agreement with the results of TEM measurements shown in Figure 1a.

Figure 3a shows the absorption spectra of particles dissolved in chloroform. The particles prepared at 350 °C exhibited an absorption shoulder originating from excitons that appeared at ca. 550 nm with absorption onset at ca. 620 nm (corresponding to an energy gap (E_g) of 2.0 eV) in both cases of $R_{Zn} = 1.0$ and 0.75. Since the E_g of bulk AZTS is 2.0 eV,[22] most of the AZTS nanoparticles possessed an energy gap similar to that of the bulk material. On the other hand, lowering of the reaction temperature below 350 °C caused broadening of the absorption spectra with red-shifting of the onset wavelength to ca. 900 nm for the particles prepared at 250 °C. Bulk ZnS has an E_g of 3.5 eV, then the absorption spectra of particles obtained were, therefore, not influenced by rod-shaped ZnS formation in the range of wavelengths longer than 360 nm. However, it has been reported

that bulk Ag_8SnS_6 material has an E_g of 1.28–1.39 eV.[25] Thus, the results indicated that Ag–Sn–S compounds having lower E_g than that of AZTS were formed at 250 °C, being in accordance with the results of XRD analyses (Figure 2).

For the use of the nanoparticles as solid devices, it is important to immobilize nanoparticles on the substrate. We accumulated AZTS nanoparticles at 350 °C with $R_{Zn} = 0.75$, which contained no impurities of ZnS and Ag_8SnS_6, via layer-by-layer deposition with the use of EDT as a linker molecule.[23] The absorption spectra of AZTS films immobilized on a quartz substrate agreed well with that of AZTS nanoparticles in the solution, and then the absorbance of the films linearly increased with an increase in the number of accumulation cycles (Figure S3[26]), indicating that the immobilization procedure did not induce any changes in the optical properties of AZTS nanoparticles and that the amount of the immobilized particles could be controlled by repeating the accumulation cycles. AFM measurements of the AZTS films prepared with five accumulation cycles revealed that the surface of the quartz substrate used was fully covered with AZTS nanoparticles (not shown). Figure 3b shows photoresponse of an AZTS nanoparticle film immobilized on an ITO substrate in an acetonitrile solution containing 0.1 mol dm^{-3} $LiClO_4$ and 10 mmol dm^{-3} triethanolamine as a hole scavenger. Irradiation to the electrodes produced an anodic photocurrent at potential application more positive than −0.67 V vs. Ag/AgCl, the magnitude being increased with a positive shift of the applied potential (Figure 3b). This behavior indicated that AZTS immobilized on ITO worked as an n-type semiconductor photoelectrode. The action spectrum of the photocurrent was obtained with potential of the electrode at 0.5 V vs. Ag/AgCl. As shown in the inset of Figure 3b, the incident photon-to-current efficiency (IPCE) spectrum agreed well with the absorption spectrum of AZTS nanoparticles in chloroform, indicating that the photoexcitation of AZTS particles caused photocurrent generation. The values of IPCE were almost unchanged after several photochemical measurements. This suggested that AZTS nanoparticles were stable under the present experimental conditions.

In the case of n-type bulk semiconductor electrodes, photogenerated electrons can diffuse inside the semiconductor, followed by injection into a contacted electrode, when applied potential is more positive than flat band potential (E_{FB}) of the semiconductor. It is reasonable to assume that the E_{FB} of semiconductor nanoparticle films corresponds to the onset potential of anodic photocurrent, being comparable to the potential of the conduction band edge (E_{CB}) in the semiconductor nanoparticle. From the onset potential of the AZTS nanoparticle film in Figure 3b, E_{CB} was estimated to be −0.67 V vs. Ag/AgCl, and then the potential of the valence band edge (E_{VB}) was +1.33 V vs. Ag/AgCl by subtracting the E_g of AZTS (2.0 eV) from E_{CB}.

In conclusion, quaternary semiconductor nanoparticles of Ag_2ZnSnS_4 (AZTS), consisting of abundant and low-toxic elements, were successfully synthesized for the first time via a wet chemical strategy at relatively lower temperature than those used in the conventional solid-phase reactions, in which the reaction temperature and the amount of added metal precursors played an important role in the purity of the resulting nanoparticles. The AZTS nanoparticles, layer-by-layer-deposited on an ITO electrode, exhibited photoelectrochemical activities similar to those of n-type semiconductor photoelectrodes. The electronic energy structure of AZTS was determined by the onset potential of anodic photocurrent and the optical energy gap. Since Cu_2ZnSnS_4 nanoparticles have been reported to have p-type semiconductor properties,[16] the layer-by-layer accumulation of p-type and n-type I–II–IV–VI semiconductor nanoparticles on the electrode will give an inorganic multilayer, the electronic energy structure of which will be adjustable for the fabrication of photovoltaic devices depending on the kind of nanoparticles and the stacked structure of particles.

This work was supported by a Funding Program for Next Generation World-Leading Researchers (NEXT Program) from the Japan Society for the Promotion of Science.

References and Notes

1 H. Mattoussi, J. M. Mauro, E. R. Goldman, G. P. Anderson, V. C. Sundar, F. V. Mikulec, M. G. Bawendi, *J. Am. Chem. Soc.* **2000**, *122*, 12142.
2 M. Han, X. Gao, J. Z. Su, S. Nie, *Nat. Biotechnol.* **2001**, *19*, 631.
3 C. Tortiglione, A. Quarta, A. Tino, L. Manna, R. Cingolani, T. Pellegrino, *Bioconjugate Chem.* **2007**, *18*, 829.
4 V. L. Colvin, M. C. Schlamp, A. P. Alivisatos, *Nature* **1994**, *370*, 354.
5 T. Nakanishi, B. Ohtani, K. Uosaki, *J. Phys. Chem. B* **1998**, *102*, 1571.
6 Y. Nosaka, *J. Phys. Chem.* **1991**, *95*, 5054.
7 T. Kiyonaga, T. Akita, H. Tada, *Chem. Commun.* **2009**, 2011.
8 P. O. Anikeeva, J. E. Halpert, M. G. Bawendi, V. Bulović, *Nano Lett.* **2009**, *9*, 2532.
9 P. V. Kamat, *J. Phys. Chem. C* **2007**, *111*, 2834.
10 A. G. Pattantyus-Abraham, I. J. Kramer, A. R. Barkhouse, X. Wang, G. Konstantatos, R. Debnath, L. Levina, I. Raabe, M. K. Nazeeruddin, M. Grätzel, E. H. Sargent, *ACS Nano* **2010**, *4*, 3374.
11 E. M. Barea, M. Shalom, S. Giménez, I. Hod, I. Mora-Seró, A. Zaban, J. Bisquert, *J. Am. Chem. Soc.* **2010**, *132*, 6834.
12 A. J. Nozik, *Physica E (Amsterdam, Neth.)* **2002**, *14*, 115.
13 W. Hu, K. Manabe, T. Furukawa, M. Matsumura, *Appl. Phys. Lett.* **2002**, *80*, 2640.
14 J. B. Sambur, T. Novet, B. A. Parkinson, *Science* **2010**, *330*, 63.
15 K. Ogisu, K. Takanabe, D. Lu, M. Saruyama, T. Ikeda, M. Kanehara, T. Teranishi, K. Domen, *Bull. Chem. Soc. Jpn.* **2009**, *82*, 528.
16 T. Kameyama, T. Osaki, K.-i. Okazaki, T. Shibayama, A. Kudo, S. Kuwabata, T. Torimoto, *J. Mater. Chem.* **2010**, *20*, 5319.
17 S. C. Riha, B. A. Parkinson, A. L. Prieto, *J. Am. Chem. Soc.* **2009**, *131*, 12054.
18 A. Khare, A. W. Wills, L. M. Ammerman, D. J. Norris, E. S. Aydil, *Chem. Commun.* **2011**, *47*, 11721.
19 C. Steinhagen, M. G. Panthani, V. Akhavan, B. Goodfellow, B. Koo, B. A. Korgel, *J. Am. Chem. Soc.* **2009**, *131*, 12554.
20 Q. Guo, H. W. Hillhouse, R. Agrawal, *J. Am. Chem. Soc.* **2009**, *131*, 11672.
21 X. Lu, Z. Zhuang, Q. Peng, Y. Li, *Chem. Commun.* **2011**, *47*, 3141.
22 I. Tsuji, Y. Shimodaira, H. Kato, H. Kobayashi, A. Kudo, *Chem. Mater.* **2010**, *22*, 1402.
23 J. M. Luther, M. Law, Q. Song, C. L. Perkins, M. C. Beard, A. J. Nozik, *ACS Nano* **2008**, *2*, 271.
24 S. Chen, A. Walsh, Y. Luo, J.-H. Yang, X. G. Gong, S.-H. Wei, *Phys. Rev. B* **2010**, *82*, 195203.
25 O. Madelung, M. Schulz, H. Weiss, *Landolt-Börnstein*, Springer, **1985**.
26 Supporting Information is available electronically on the CSJ-Journal Web site, http://www.csj.jp/journals/chem-lett/index.html.

